

# *Causality in the winter interaction between extratropical storm tracks, atmospheric circulation, and Arctic sea ice loss*

Article

Published Version

Creative Commons: Attribution 4.0 (CC-BY)

Open Access

Mousavizadeh, M., Alizadeh, O., Hodges, K. I. ORCID: <https://orcid.org/0000-0003-0894-229X> and Simmonds, I. (2025) Causality in the winter interaction between extratropical storm tracks, atmospheric circulation, and Arctic sea ice loss. *Journal of Geophysical Research: Atmospheres*, 130 (5). e2024JD042128. ISSN 2169-8996 doi: <https://doi.org/10.1029/2024JD042128> Available at <https://centaur.reading.ac.uk/120941/>

It is advisable to refer to the publisher's version if you intend to cite from the work. See [Guidance on citing](#).

To link to this article DOI: <http://dx.doi.org/10.1029/2024JD042128>

Publisher: American Geophysical Union

All outputs in CentAUR are protected by Intellectual Property Rights law, including copyright law. Copyright and IPR is retained by the creators or other copyright holders. Terms and conditions for use of this material are defined in the [End User Agreement](#).

[www.reading.ac.uk/centaur](http://www.reading.ac.uk/centaur)

**CentAUR**

Central Archive at the University of Reading

Reading's research outputs online

# JGR Atmospheres

## RESEARCH ARTICLE

10.1029/2024JD042128

### Key Points:

- Recent cooling trend in northeastern Asia occurs in the midtroposphere, primarily driven by sea ice loss in the Barents-Kara Sea (BKS)
- Changes in atmospheric circulation are unlikely to be the primary driver of recent sea ice loss in the BKS
- In atmosphere-driven winters, amplified surface warming in the Barents-Kara and Chukchi Seas result from storm-driven warm air advection

### Supporting Information:

Supporting Information may be found in the online version of this article.

### Correspondence to:

O. Alizadeh,  
[omid.alizadeh@hu-berlin.de](mailto:omid.alizadeh@hu-berlin.de)

### Citation:

Mousavizadeh, M., Alizadeh, O., Hodges, K. I., & Simmonds, I. (2025). Causality in the winter interaction between extratropical storm tracks, atmospheric circulation, and Arctic sea ice loss. *Journal of Geophysical Research: Atmospheres*, 130, e2024JD042128. <https://doi.org/10.1029/2024JD042128>

Received 4 AUG 2024

Accepted 15 FEB 2025

### Author Contributions:

#### Conceptualization:

Morteza Mousavizadeh, Omid Alizadeh

**Formal analysis:** Morteza Mousavizadeh

**Investigation:** Morteza Mousavizadeh, Omid Alizadeh

**Methodology:** Morteza Mousavizadeh, Omid Alizadeh, Kevin I. Hodges

**Supervision:** Omid Alizadeh

**Visualization:** Morteza Mousavizadeh

**Writing – original draft:**

Morteza Mousavizadeh

**Writing – review & editing:**

Morteza Mousavizadeh, Omid Alizadeh,

Kevin I. Hodges, Ian Simmonds

© 2025. The Author(s).

This is an open access article under the terms of the [Creative Commons Attribution License](https://creativecommons.org/licenses/by/4.0/), which permits use, distribution and reproduction in any medium, provided the original work is properly cited.

# Causality in the Winter Interaction Between Extratropical Storm Tracks, Atmospheric Circulation, and Arctic Sea Ice Loss

Morteza Mousavizadeh<sup>1</sup> , Omid Alizadeh<sup>2</sup> , Kevin I. Hodges<sup>3</sup> , and Ian Simmonds<sup>4</sup> 

<sup>1</sup>Institute of Geophysics, University of Tehran, Tehran, Iran, <sup>2</sup>Geography Department, Humboldt-Universität zu Berlin, Berlin, Germany, <sup>3</sup>Department of Meteorology and National Centre for Atmospheric Science, University of Reading, Reading, UK, <sup>4</sup>School of Geography, Earth and Atmospheric Sciences, University of Melbourne, Melbourne, VIC, Australia

**Abstract** Global warming is accelerating the decline of Arctic sea ice, with wide-ranging impacts on the Earth's climate system. Using ERA5 data from 1980 to 2023, we investigated the relationship between winter extratropical storm tracks, atmospheric circulation patterns, and sea ice area (SIA) in three key Arctic regions. We classified the winters into two categories: atmosphere-driven winters (ADWs), when atmospheric circulation influences sea ice, and ice-driven winters (IDWs), when sea ice influences atmospheric circulation. This classification was based on the sign of SIA and surface turbulent heat flux anomalies in the Barents-Kara Sea (BKS), Baffin Bay, Davis Strait, and Labrador Sea (BDL), and Chukchi-Bering Seas (CBS). Our findings show that in IDWs, reduced SIA has a minor effect on extratropical storm tracks. However, we observed significant midtropospheric cooling over northeastern Asia, aligning with the effects of reduced ice in the BKS during IDWs. This emphasizes the importance of considering the entire tropospheric temperature profile to capture the impact of sea ice loss. In contrast, during ADWs, the BKS and CBS regions experience amplified surface warming and SIA loss due to storm-induced intrusion of warm and moist air, with sea ice loss in the BKS contributing to strengthening Ural blocking. Although cyclone-induced heat and moisture intrusion is prevalent, we found no significant trend in track density or mean intensity of positive V extrema in the North Atlantic sector of the Arctic, suggesting that changes in atmospheric circulation are unlikely to be the driver of recent sea ice loss in the BKS.

**Plain Language Summary** Global warming is causing Arctic sea ice to shrink, which affects the Earth's climate in many ways. Using ERA5 data from 1980 to 2023, we studied how changes in storm patterns, atmospheric conditions, and sea ice are connected in three Arctic regions. We classified winters into two categories: atmosphere-driven winters (ADWs), in which atmospheric conditions affect sea ice, and ice-driven winters (IDWs), in which sea ice influences atmospheric conditions. We found that during IDWs, sea ice loss has only a small effect on storm patterns, but it leads to cooling in the midatmosphere over northeastern Asia. This highlights the need to look at temperature changes throughout the entire atmosphere, not just at the surface. In ADWs, storm-driven warm, moist air leads to more surface warming and sea ice loss, particularly in the Barents-Kara Sea, where the sea ice loss also contributes to stronger Ural blocking. Although storms in these regions bring heat and moisture, we did not find a clear trend in the number or intensity of storms, suggesting that changes in atmospheric circulation are not the main cause of recent sea ice loss. This research helps to better understand how Arctic sea ice loss and atmospheric changes are linked.

## 1. Introduction

The Arctic has been warming at a much faster rate than other regions (Alizadeh & Lin, 2021; Rantanen et al., 2022), and this has been accompanied by substantial sea ice loss (Simmonds & Li, 2021; Stroeve & Notz, 2018). The rapid Arctic warming has led to a reduced meridional temperature gradient between the Arctic and midlatitudes, contributing to weaker and more meandering jet streams (Alizadeh et al., 2024; Francis & Vavrus, 2015; Luo et al., 2024), less frequent storms (Hay et al., 2023), and slower propagation of Rossby waves (Francis & Vavrus, 2012).

Among the various processes driving this amplified Arctic warming, the positive surface albedo feedback stands out as a principal driver (Hall, 2004; Serreze et al., 2009). As sea ice melts, it exposes darker ocean surfaces that

absorb more solar radiation, further amplifying the warming process. Other important factors include smaller blackbody emissions per unit of warming in the Arctic than lower latitudes, due to its colder temperatures (Jenkins & Dai, 2021). The Arctic also experiences a stronger positive lapse rate feedback due to a larger warming of the surface and lower troposphere than in the middle and upper troposphere (Pithan & Mauritsen, 2014). Furthermore, positive longwave cloud radiative feedback is another key factor driving the rapid Arctic warming (Gong et al., 2017; Lee et al., 2017). Enhanced heat (Asbjørnsen et al., 2020; Cai, 2006; Graversen & Burtu, 2016) and moisture (Woods & Caballero, 2016) transport, along with changes in oceanic heat content (Årthun et al., 2019; Ivanov et al., 2016) have also played a role in rapid Arctic warming.

Moisture and atmospheric heat transport into the Arctic mainly occur through the intrusion of warm, moist air linked to extratropical cyclones (Dufour et al., 2016; Fearon et al., 2021; Sorteberg & Walsh, 2008) and Rossby wave breaking (Liu & Barnes, 2015). Extratropical cyclones primarily enter the Arctic through three major pathways of the North Pacific, the Labrador Sea, and especially the North Atlantic (Dufour et al., 2016; Woods et al., 2013). In winter, the absence of shortwave radiation in the Arctic, coupled with enhanced extratropical cyclone activity, promotes the importance of these cyclones and their associated storm tracks in influencing the Arctic sea ice extent.

Thinner sea ice is more susceptible to melting and to the effects of stronger winds and waves associated with cyclones (Zhang et al., 2013). As such, the thinning of sea ice in response to rapid Arctic warming in recent decades is expected to amplify the impact of cyclones on Arctic sea ice (Simmonds et al., 2008; Simmonds & Keay, 2009). Several studies have indicated that cyclonic activity in the high latitudes of the Northern Hemisphere (NH) has changed in recent decades, with a notable decrease in winter and an increase in summer (e.g., Day et al., 2018; Rinke et al., 2017; Zahn et al., 2018) due to alterations in the meridional temperature gradient (Day et al., 2018).

The retreat of the Arctic sea ice enhances the transfer of energy and moisture from the ocean to the atmosphere through upward surface turbulent heat flux (STHF), which plays a crucial role in shaping regional climate patterns and atmospheric circulation (Ahmadi & Alizadeh, 2023; Deser et al., 2010). For example, the anomalous STHF over the Barents-Kara Sea (BKS) in late autumn triggers a stationary Rossby wave train that strengthens the Siberian High in winter, thereby intensifying northerly cold air advection over Eastern Eurasia in early winter (Honda et al., 2009). Additionally, the anomalous STHF over the BKS significantly influences near-surface meridional temperature gradients and zonal winds (Oутten & Esau, 2012; Petoukhov & Semenov, 2010), which in turn affect cyclone pathways and the formation of cold anticyclonic flow anomalies north of the Eurasian continent (Inoue et al., 2012). In some winters, however, the anomalous STHF from the ocean to the atmosphere, linked to reduced sea ice in some Arctic regions, is accompanied by anomalous STHF from the atmosphere to the ocean on the equatorward side of the ice edge. This bipolar surface turbulent flux pattern is caused by the poleward advection of warm air into the sea ice-covered region. Such a warm air intrusion into the sea ice-covered area reflects the internal variability of the winter atmospheric circulation (Deser et al., 2000).

Blackport et al. (2019) employed an approach based on the signs of sea ice area (SIA) and STHF anomalies over the BKS and Chukchi-Bering Seas (CBS) to examine the impact of sea ice loss in these regions on NH surface temperature and sea level pressure. They defined “ice-driven winters” (IDWs) as those in which the anomalies of SIA and STHF have opposite signs, and “atmosphere-driven winters” (ADWs) as those in which the anomalies have the same sign. In IDWs, positive SIA anomalies induce negative STHF anomalies (with STHF from the atmosphere to the ocean being positive), and vice versa (i.e., negative SIA anomalies lead to positive STHF anomalies). In contrast, during ADWs, moist southerly airflow decreases SIA and creates a downward STHF anomaly, while an increase in SIA is associated with an upward STHF anomaly. Blackport et al. (2019) focused on surface conditions, using sea level pressure and surface air temperature, and observed that reduced Arctic sea ice had minimal influence on coincident cold winters in midlatitudes. While their analysis based on surface-level fields provides valuable insights, a broader perspective extending into the troposphere may reveal additional findings.

There is ongoing debate about the relationship between winter cooling over continents and Arctic sea ice reduction. Some studies suggest that decreased sea ice can lead to colder winters in Eurasia (e.g., Mori et al., 2014, 2019; Tang et al., 2013; Xu et al., 2023), while others find no such connection (e.g., Blackport et al., 2019; Dai & Song, 2020). Zhuo et al. (2023) highlight that the nature of these connections may vary depending on the specific region of the Arctic considered. Some studies indicate that stratosphere-troposphere coupling in model simulations is crucial for the stronger response of atmospheric circulation to sea ice reduction (e.g., Xu et al., 2023;

Zhang et al., 2018). Furthermore, accurately capturing the physical processes associated with sea ice-induced turbulent heat flux (THF) anomalies in models is essential (Yu et al., 2024). Thus, dismissing the influence of sea ice reduction on cold continental winters based on model experiments may be questionable. Many studies reporting minimal impacts of sea ice decline on Eurasian winters focus primarily on near-surface temperatures. In contrast, more recent studies have extended their analysis beyond the surface (e.g., He et al., 2020; Xie et al., 2020; Xu et al., 2023). For example, Xie et al. (2020) showed that Arctic warming influences Eurasian cooling at both the surface and midtroposphere by examining potential vorticity dynamics. He et al. (2020) found that Eurasian winter cooling is more pronounced during periods of deep warming than shallow warming in areas with reduced sea ice. However, they also demonstrated that this deep warming is driven by moisture and energy transport from the North Atlantic into the Arctic, rather than by sea ice decline. Xu et al. (2023) showed that when stratosphere-troposphere coupling is considered in model simulations, sea ice reduction can lead to deeper warming. Therefore, while studies like Blackport et al. (2019) focus on surface conditions, adopting a broader perspective that includes the entire troposphere may reveal new insights.

This study investigates the causal interactions between extratropical storm tracks, atmospheric circulation patterns, and regional Arctic SIA in winter using data from the European Centre for Medium-Range Weather Forecasts (ECMWF) 5th generation reanalysis (ERA5). Our study addresses the following key questions: (a) What is the relationship between reduced regional sea ice in the Arctic, extratropical cyclones, and atmospheric circulation on an interannual timescale during winter? (b) What is the primary cause of cold midlatitude winters: atmospheric circulation or Arctic sea ice reduction? (c) Has Arctic sea ice loss in recent decades been influenced by an increase in storm-induced heat and moisture intrusion into the Arctic?

To answer these questions, we adopted the same approach as Blackport et al. (2019), analyzing geopotential height at 850 hPa and 1,000 and 500 hPa geopotential thickness. Moreover, to explore the relationship between storm tracks and sea ice, we extended our analysis to include track density and mean intensity, computed by tracking positive V850 wind, which serves as a proxy for the northward transport of warm and moist air on the eastern side of cyclones.

## 2. Data Description and Methodology

We used ERA5 data (Hersbach et al., 2020) for winter (December-January-February, DJF) spanning the period from 1979/1980 to 2022/2023, referred to hereafter as 1980–2023. The analysis utilized 3-hourly data with a horizontal resolution of T128 (triangular truncation at 128 on a Gaussian grid) and monthly products with a  $0.5^\circ \times 0.5^\circ$  resolution for the cyclone tracking and regression analysis, respectively. To diagnose storm tracks in the NH, we applied a Lagrangian feature tracking approach of Hodges (1994, 1995, 1999). This method has been extensively applied to detect storm tracks using both reanalysis data (e.g., Hoskins & Hodges, 2002, 2005, 2019a, 2019b) and model simulations (e.g., Bengtsson et al., 2006, 2009; Catto et al., 2011; Zappa et al., 2013).

Of the fields used by Hoskins and Hodges (2002), we selected the positive meridional wind component ( $V$ ) at 850 hPa to diagnose storm tracks. This variable is proportional to the zonal derivative of geopotential (or pressure). While tracking  $V$  extrema may not accurately detect small synoptic systems compared to relative vorticity, it outperforms in this regard compared to tracking mean sea level pressure (Hoskins & Hodges, 2019a). Furthermore, this method can capture an essential aspect of baroclinic cyclone growth (Hoskins and Hodges, 2019a, 2019b). Positive  $V$  extrema indicate poleward advection of warm air in the east of a cyclone center, while negative extrema represent equatorward advection of cold air in the west. In line with this, Clancy et al. (2022) demonstrated that sea ice decreases east of a cyclone and increases to the west. Thus, tracking positive  $V$  extrema, particularly in the sub-Arctic and Arctic regions, reveals the storm-induced intrusion of warm air into these regions, making it a valuable tool for investigating the impact of extratropical cyclones on Arctic sea ice melting.

To detect the storm tracks, we spectrally smoothed  $V$  on a T42 Gaussian grid by removing spectral components with total wave numbers larger than 42 (to filter out small-scale noise) and smaller than 6 (to eliminate the large-scale background field), ensuring that only synoptic-scale features are considered. Storm features were identified as relative maxima in the filtered field on a polar stereographic projection, with the meridional wind component exceeding  $1 \text{ m s}^{-1}$  (i.e., positive  $V$  extrema). Once the extrema were detected, we traced their path directly on the unit sphere, following methods similar to those in previous studies (e.g., Hoskins & Hodges, 2019a, 2019b). The tracks were then filtered to retain only mobile features that lasted at least 2 days (16 time steps) and traveled more than 1,000 km. These filters are consistent with the propagating nature of extratropical cyclones and help exclude

unrealistic short-lived or stationary features (Zappa et al., 2013), allowing to focus on the mobile systems with the greatest climate impact (Bengtsson et al., 2006). Finally, we computed storm track density and mean intensity from the ensemble of filtered tracks for each monthly period using the spherical kernel method (Hodges, 1996). Track density is determined as the number of features per unit area per month, with the unit area corresponding to a  $5^\circ$  spherical cap (approximately  $10^6 \text{ km}^2$ ), and mean intensity is given in  $\text{m s}^{-1}$  for the meridional wind component.

We adopted the same methodology as Blackport et al. (2019). Our focus was on the BKS, the Baffin Bay, Davis Strait, and Labrador Sea (BDL), and CBS in the Arctic, as these areas exhibit significant sea ice variability during winter. Initially, we calculated the SIA for the regions of interest for each winter season, and then detrended the resulting time series for the period from 1980 to 2023. We standardized the time series of SIA, such that regression maps represent the field associated with one standard deviation in the SIA. Prior to conducting the regression analysis, we reversed the sign of the SIA, so that the regression would reflect a one standard deviation reduction in SIA. Subsequently, we classified each winter into either IDWs, where SIA and STHF anomalies exhibit opposite signs, or ADWs, where they show the same sign. The number of IDWs and ADWs varied across regions (see Figure S1 in Supporting Information S1). In the BKS region, 30 winters were classified as IDWs (with an SIA standard deviation of 1.07), while 14 were classified as ADWs (with an SIA standard deviation of 0.75). In the CBS region, 18 winters were IDWs (SIA standard deviation: 0.85), and 27 were ADWs (SIA standard deviation: 1.10). In the BDL region, 21 winters were IDWs (SIA standard deviation: 1.03), and 23 were ADWs (SIA standard deviation: 0.96).

We applied linear detrending to the seasonal averages of the track density, mean intensity of cyclones, geopotential height, both components of wind at 850 hPa, and geopotential thickness between 1,000 and 500 hPa. These seasonal fields were then linearly regressed onto the standardized SIA indices, with the sign reversed as described earlier. After classifying the seasonal fields into the two regimes, IDWs and ADWs, linear regression was performed for each regime separately.

To assess the robustness of our findings, we also performed 1-month lead-lag linear regression analyses with the standardized SIA indices, offering an independent approach to examine causality. The 1-month lead and lag in our analysis correspond to SIA indices calculated from the 3-month averages of November-December-January (NDJ) and January-February-March (JFM), respectively. We tested the statistical significance of the regressions using a two-tailed Student's  $t$  test and a Monte Carlo test with 1,000 permutations, which yielded similar results. To control for false positives in Figures 2 and 5, and S2 in Supporting Information S1, we applied the false discovery rate (FDR) (Wilks, 2016).

### 3. Results

#### 3.1. The Barents-Kara Sea

Regression analysis reveals that the geopotential height pattern associated with reduced sea ice in all winters in the BKS ( $30\text{--}150^\circ\text{E}$ ,  $70\text{--}85^\circ\text{N}$ ) exhibits an anticyclonic anomaly over the BKS and northern Russia (Figure 1a), indicating the strengthening and persistence of Ural blocking. This anomalous blocking, characterized by strong anticyclonic winds, facilitates the advection of cold air from the Arctic into northeastern Asia and the advection of warm air from lower latitudes into the BKS. Furthermore, geopotential thickness in northeastern Asia is significantly reduced (Figure 1a), suggesting a cooling of this region from the midtroposphere to the upper troposphere.

The reduced sea ice in the BKS during IDWs (68% of all winters) is associated with an anticyclonic geopotential height anomaly over the BKS, extending toward the Norwegian and Greenland Seas (Figure 1b). This anomaly, along with its associated anticyclonic winds, leads to the advection of cold air into northeastern Asia. In contrast, reduced sea ice in ADWs (32% of all winters) is linked to a strong anticyclonic geopotential height anomaly over northern Russia, which drives the transport of cold air from the Arctic to northeastern Asia (Figure 1c). Additionally, a pronounced positive North Atlantic Oscillation (NAO) pattern develops (Figure 1c), facilitating the advection of warm and moist air from the North Atlantic into the BKS through the Greenland and Norwegian Seas (Luo et al., 2017; Sato et al., 2014; Simmonds & Govekar, 2014; Woods et al., 2013).

Based on model analysis, Sato et al. (2014) concluded that the warming of the Gulf Stream can generate a planetary wave train structure across the North Atlantic and Eurasia. This wave train is characterized by stronger anticyclonic anomaly in the North Atlantic, a cyclonic anomaly over the North Atlantic sector of the Arctic, and a

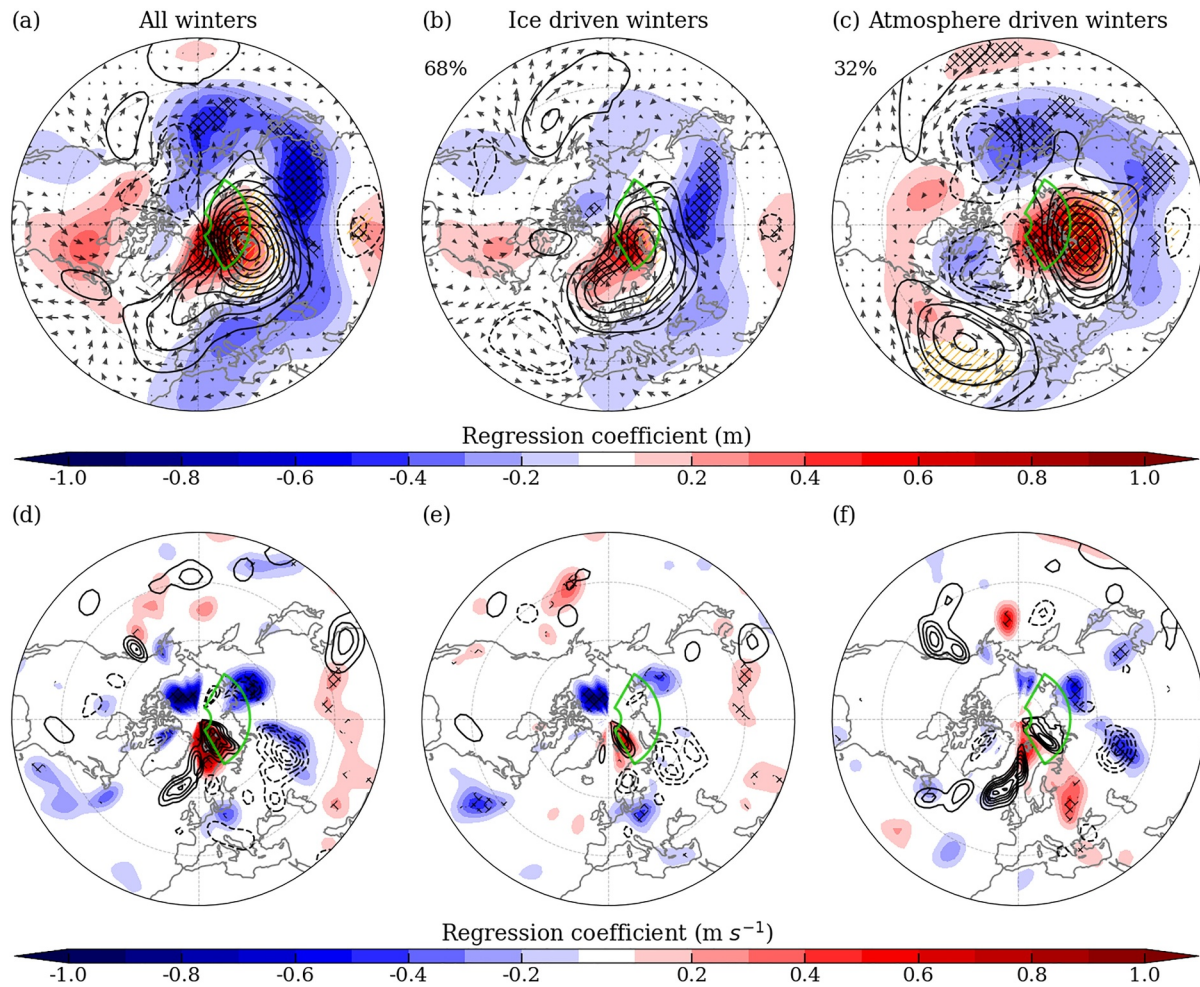


**Figure 1.** Geopotential height at 850 hPa (contours, 2-m intervals) and geopotential thickness between 1,000 and 500 hPa (shading, 2-m intervals) regressed on standardized reduced sea ice area (SIA) in the Barents-Kara Sea (BKS) (30–150°E, 70–85°N, shown by the green polygon) for (a) all winters, (b) ice-driven winters (IDWs), and (c) atmosphere-driven winters (ADWs). Cyclone track density (contours, 0.3 number density per unit area per month) and mean intensity (shading, 0.1 m s<sup>-1</sup> intervals) regressed on standardized reduced SIA for (d) all winters, (e) IDWs, and (f) ADWs. SIA is reversed to represent a 1 standard deviation reduction. Solid/dashed contours indicate positive/negative values (zero contour not shown). In panels (a–c), gold/black hatching denotes significance at the 95% confidence level for geopotential height/thickness. Percentages of IDWs and ADWs are shown in the top left of panels (b) and (c). In panels (d–f), track density is shown where regression is significant at the 95% confidence level, and mean intensity is shown at the 90% confidence level (95% confidence level is indicated by hatching). Regression coefficients for IDWs/ADWs are multiplied by their respective ratios.

stronger anticyclonic anomaly in the BKS and northern Eurasia. Their findings suggest that the local response to reduced sea ice in the BKS cannot directly trigger such a wave train structure, but could amplify the remote response of the Gulf Stream. Therefore, Ural blocking is influenced not only by the direct impact of reduced sea ice in the BKS but also by the warming of the midlatitude North Atlantic.

Our results indicate that due to the absence of a positive NAO-like pattern in IDWs, there is no advection of warm and moist air from the North Atlantic into the Arctic. Furthermore, the wave train structure across the Eurasian continent, originating from the North Atlantic, is not present. This suggests that the reduced ice in the BKS in IDWs can only advect cold air into northeastern Asia by locally promoting Ural blocking. The absence of a positive NAO pattern in IDWs in our study (Figure 1b) is consistent with the results of Sato et al. (2014), who demonstrated that the warming of the BKS cannot directly induce a positive NAO pattern. However, the warm Arctic and cold Asia pattern observed in IDWs (Figure 1b) can be attributed to the reduction of westerly winds in the middle and high latitudes of Asia (Figure 1b), which favors the persistence of Ural blocking (Luo et al., 2016).

Based on the approach of Blackport et al. (2019), the regression coefficients between the BKS ice and surface air temperature in Asia are significantly larger in ADWs than IDWs. They concluded that the reduction in BKS ice is

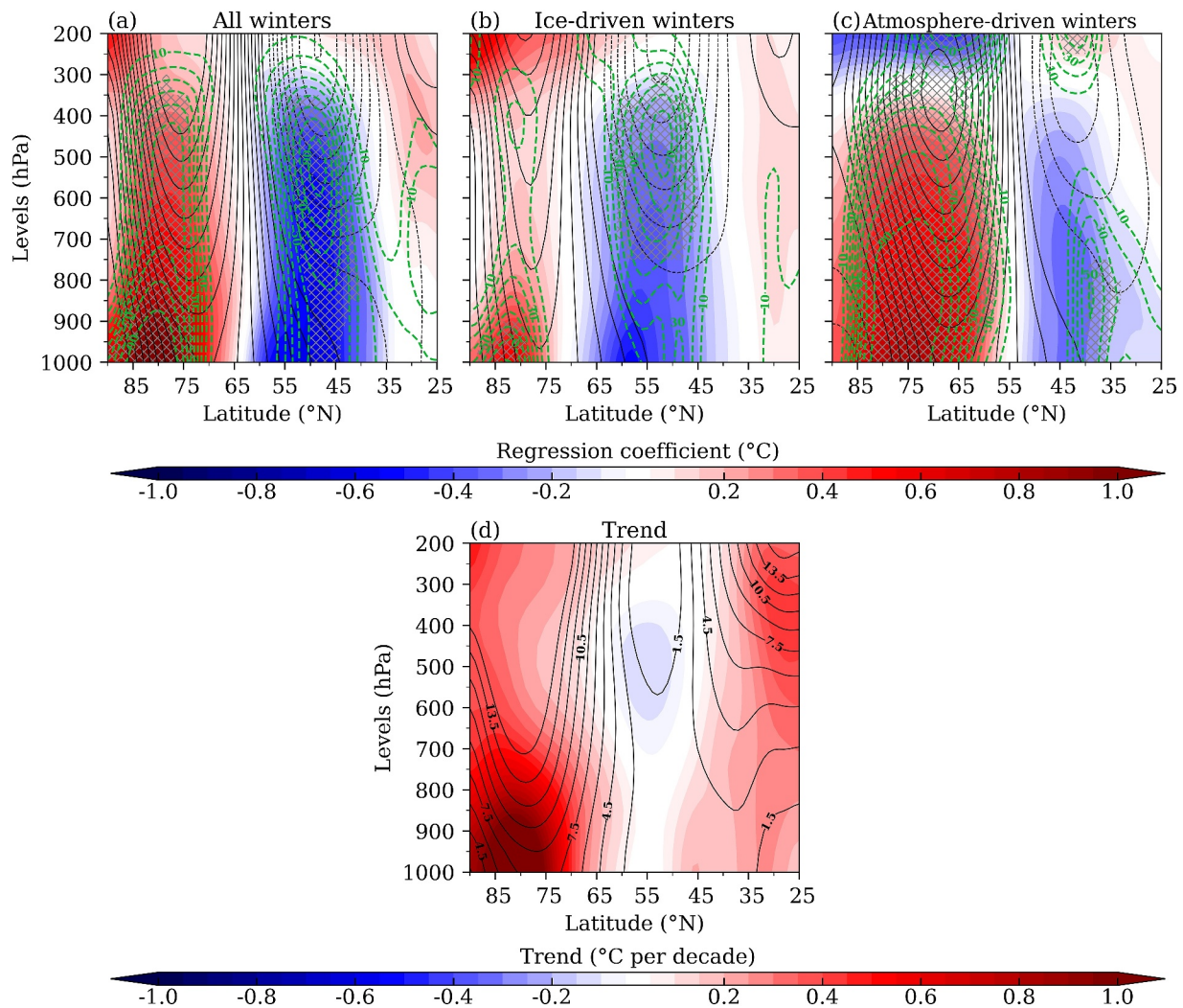


**Figure 2.** Latitude-height cross-sections of geopotential height (contours, 1.5-m intervals) and temperature (shading, 0.05-K intervals) in Asia (70–130°E, 25–90°N) regressed on standardized reduced sea ice area (SIA) in the Barents-Kara Sea (BKS) for (a) all winters, (b) ice-driven winters (IDWs), and (c) atmosphere-driven winters (ADWs), and (d) linear trends of geopotential height (contours, 1.5 m per decade) and temperature (shading, 0.05 K per decade) in Asia. Green dotted lines and hatching indicate temperature significance at the 95% level and areas with at least 20% of grid points significant after false discovery rate correction ( $\alpha_{FDR} = 0.1$ ), respectively. The sign of SIA is reversed to represent a 1 standard deviation reduction. Solid/dashed contours indicate positive/negative values (zero contour not shown). Regression coefficients for IDWs/ADWs are multiplied by their respective ratios.

not the primary cause of the recent cooling trend in northeastern Asia. However, the analysis of geopotential thickness between 1,000 and 500 hPa reveals that the cooling of northeastern Asia associated with the reduced SIA in the BKS is more pronounced during IDWs and is primarily statistically significant from the midtroposphere to the upper troposphere rather than at the surface (Figures 1b and 1c).

Considering the classification of winters into atmosphere-driven and ice-driven regimes, based on the sign of SIA and STHF anomalies, we observe that on subseasonal timescales in an IDW, the reduction in sea ice in the BKS can lead to an anticyclonic geopotential height anomaly over the BKS and cooling in the midtroposphere in northeastern Asia. However, this anticyclonic anomaly can further accelerate sea ice loss through a downward THF. To assess the potential impact of such feedback loops on our findings, we conducted 1-month lead-lag regressions. One month after the reduction in sea ice (Figure S2b in Supporting Information S1), the geopotential height and geopotential thickness patterns resemble those observed during IDWs (Figure 1b). In contrast, 1 month ahead of reduced sea ice (Figure S2c in Supporting Information S1), the geopotential height and geopotential thickness patterns resemble those seen during ADWs (Figure 1c). The consistency between our lead-

lag analysis and the physical classification based on the sign of STHF and SIA anomalies strengthens the robustness of our findings. Therefore, the physical classification of winters, particularly in the BKS, can reliably identify whether sea ice is primarily driving the atmospheric circulation or whether the atmosphere is driving sea ice during winter.

The most pronounced warming associated with reduced sea ice in the BKS in all winters occurs at high latitudes ( $>70^{\circ}\text{N}$ ) near the surface (Figure 2a), while the maximum cooling of northeastern Asia is observed in the midtroposphere (around 500 hPa) at approximately  $40\text{--}60^{\circ}\text{N}$ . In IDWs, reduced sea ice is associated with much less surface warming than that observed above  $70^{\circ}\text{N}$  in all winters (Figures 2a and 2b). Another distinction is that cooling in IDWs occurs between  $45$  and  $65^{\circ}\text{N}$ , with statistical significance from the midtroposphere to the upper troposphere. In contrast, in ADWs (Figure 2c), significant warming is observed north of  $60^{\circ}\text{N}$ , extending from near the surface to the upper troposphere, along with notable cooling of Asia from the near-surface to the midtroposphere at around  $35\text{--}50^{\circ}\text{N}$ . Blackport et al. (2019) found stronger Asian cooling during ADWs than IDWs based on the analysis of sea level pressure and surface air temperature. However, our results show that the signal of the reduced BKS ice during IDWs is more prominent from the midtroposphere to the upper troposphere. The analysis of temperature trends also indicates that cooling in midlatitude Asia is much stronger in the midtroposphere than at the surface (Figure 2d).

Both 1 month after (Figure S3b in Supporting Information S1) and 1 month prior to (Figure S3c in Supporting Information S1) the observed reduction in the BKS ice, the patterns of geopotential height and temperature resemble those observed during ice-driven (Figure 2b) and atmosphere-driven (Figure 2c) winters, respectively. The key difference lies in the spatial distribution of points with statistically significant regressions of temperature onto the standardized reduced SIA in the BKS. One month after the sea ice reduction (Figure S3b in Supporting Information S1), statistically significant regression points for temperature are found both at the surface and in the midtroposphere around  $55^{\circ}\text{N}$ . However, one month before the sea ice reduction (Figure S3c in Supporting Information S1), statistically significant regression points are primarily confined to the midtroposphere around  $45^{\circ}\text{N}$ . Notably, one month after the sea ice reduction in the BKS, the maximum Asian cooling during IDWs occurs at the same latitude ( $55^{\circ}\text{N}$ ) where the maximum Asian cooling trend is observed (Figure 2d). This suggests a potential influence of the BKS ice loss in recent decades on Asian winter cooling.

We now turn to examine the cyclone behavior in the two types of winter and their implications for atmospheric transport. In all winters with reduced sea ice in the BKS, there is an increase in track density over the Greenland and Norwegian Seas, which serves as the primary pathway for poleward transport of energy and moisture (Figure 1d). In contrast, track density decreases over Eurasia, spanning from Europe to the Ural-Siberia region and extending into the Laptev Sea. This decrease is linked to wind anomalies that hinder the propagation of storms toward these areas. Additionally, the mean intensity of positive V extrema is enhanced over the Barents, Greenland, and Norwegian Seas, but reduced over the eastern Ural-Siberia region and south of the Laptev Sea.

In IDWs associated with reduced sea ice, there is no increase in track density poleward of the North Atlantic storm track (Figure 1e). Instead, a more localized increase in track density is observed in the Barents Sea, consistent with the warming induced by sea ice reduction, while track density decreases over the Scandinavian Peninsula, the Ural Mountains, and the Laptev Sea. This decrease is due to the prevention of warm air intrusion into the south and east of the ice-driven Ural blocking. In contrast, in ADWs associated with reduced sea ice, there is a substantial increase in track density poleward of the North Atlantic storm track, extending from the south of Greenland into the BKS (Figure 1f). This is linked to a strong positive NAO pattern, which facilitates the intrusion of warm and moist air into the BKS, further promoting sea ice loss. Conversely, track density decreases from the southern Europe to the north of the Ural-Siberia region, driven by westerly wind anomalies associated with a strong anticyclonic circulation over northern Russia and southerly winds over Europe due to a robust anticyclonic circulation over the North Atlantic (Figure 1f). The decrease in track density from southern Europe to the northern Ural-Siberia region restricts the intrusion of warm air, contributing to colder winters. Both 1 month after (Figure S2e in Supporting Information S1) and 1 month before (Figure S2f in Supporting Information S1) the observed reduction in the BKS ice, the patterns of track density and mean intensity of storms resemble those observed during ice-driven (Figure 1e) and atmosphere-driven (Figure 1f) winters, respectively. This consistency supports the physical classification approach, indicating that our findings remain robust despite potential consequences of feedback loops.

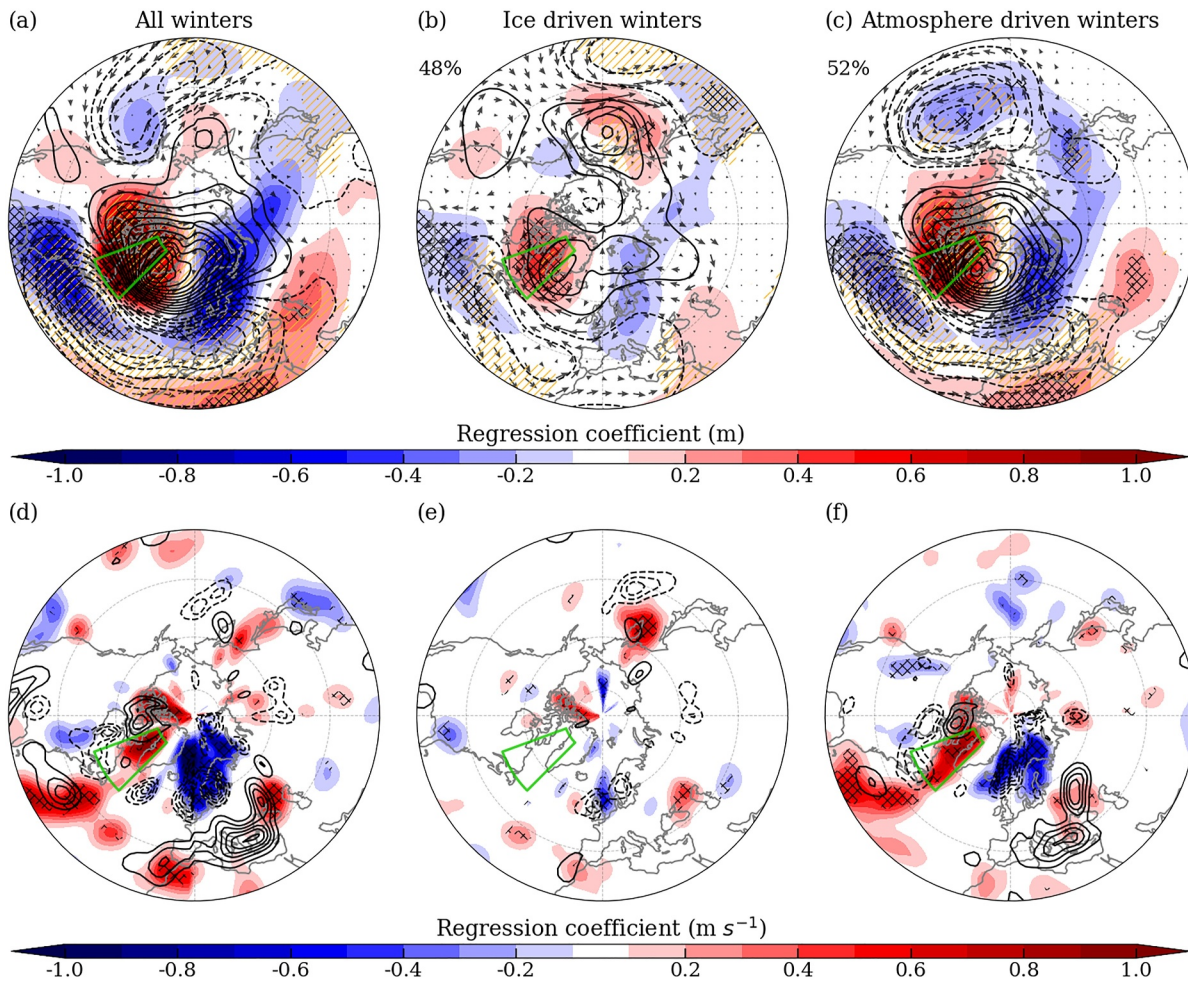


**Figure 3.** Same as Figure 1, but regressed on standardized reduced sea ice area (SIA) in the Baffin Bay, Davis Strait, and Labrador Sea (BDL) (45–70°W, 50–75°N, shown by the green polygon).

In ADWs (Figure 1f), reduced sea ice is linked to a pronounced intrusion of warm and moist air from the North Atlantic into the Arctic, facilitated by extratropical cyclones traveling through the Atlantic sector. This leads to sea ice loss, which amplifies warming over the BKS. This underscores the critical role of extratropical cyclones in sea ice loss in the BKS via the Atlantic sector. The storm-induced warming in the BKS strengthens Ural blocking and promotes the wave train structure in ADWs (Figure 1c). In contrast, in IDWs (Figure 1e), the influence of the BKS ice loss on storm tracks does not extend toward the North Atlantic and Eurasia. Instead, it favors the transport of cold air from the Arctic into northeastern Asia due to intensified Ural blocking.

### 3.2. Baffin Bay, Davis Strait, and Labrador Sea

In all winters associated with reduced sea ice in the BDL region (45–70°W, 50–75°N), a strong dipole structure of geopotential height anomalies is observed, resembling the negative phase of the NAO (Figure 3a). This pattern features an anticyclonic anomaly centered over Greenland and a cyclonic anomaly centered over the eastern North Atlantic (Figure 3a). The anticyclonic anomaly advects cold Arctic air into northern Europe, while bringing warm and moist oceanic air into both the BDL region and the high latitudes of North America. Additionally, the anticyclonic anomaly transports moist and warm air into North Africa and West Asia, while cold air is advected toward the east coast of North America and the western North Atlantic. A weak cyclonic anomaly is also observed over the central to eastern North Pacific.

In IDWs (Figure 3b; 48% of all winters), the atmospheric circulation associated with reduced sea ice in the BDL exhibits a weakly negative NAO pattern, with localized warming and nonlocal cooling in the western North

Atlantic. However, the cooling in IDWs is weaker (Figure 3b) than that observed in all winters (Figure 3a). In contrast, in ADWs (52% of all winters), the atmospheric circulation linked to reduced sea ice in the BDL shows a strong negative NAO pattern (Figure 3c), similar to that observed in all winters (Figure 3a), along with a pronounced cyclonic anomaly over the eastern North Pacific. Notably, this wave train structure is absent in IDWs. Additionally, we found smaller regression coefficients in IDWs than ADWs in the BDL, suggesting that BDL sea ice loss has a weaker influence on atmospheric circulation in IDWs.

Associated with reduced sea ice in all winters, storm track activity decreases in regions with easterly wind anomalies, particularly over the Scandinavian Peninsula and the Norwegian and Barents Seas (Figure 3d). South of the cyclonic circulation over the North Atlantic, storm track activity increases due to westerly wind anomalies. An increase in storm track activity is also observed over the western part of the anticyclone centered over Greenland. The regions to the west and the east of an anticyclonic anomaly are generally characterized by positive and negative storm track activity anomalies, respectively. A strong increase in storm activity over the western part of the anticyclone centered over Greenland contributes to sea ice loss in these regions, leading to pronounced warming. Conversely, a strong decrease in storm activity to the east of the anticyclone favors the growth of sea ice and results in more cooling. The pattern of storm activity associated with reduced sea ice in ADWs (Figure 3e) is similar to that of all winters (Figure 3d), suggesting that sea ice loss in the BDL does not significantly alter storm tracks in the NH.

### 3.3. The Chukchi-Bering Seas

The geopotential height pattern associated with reduced sea ice in all winters in the CBS (165°E and 155°W, 55 and 70°N) (Figure 4a) displays a dipole structure, with anticyclonic over the eastern CBS and cyclonic anomalies over the western CBS. This pattern facilitates the advection of warm and moist air from the North Pacific into the CBS, contributing to sea ice reduction. Additionally, the region experiences strong warming over the CBS, weaker yet statistically significant warming over the eastern North Pacific, and pronounced cooling over North America.

In IDWs (Figure 4b; 39% of all winters), the atmospheric circulation associated with reduced sea ice does not lead to warming over the CBS, northern North America, and Asia, except for a cyclonic circulation centered south of the Bering Sea, which is linked to the deepening of the Aleutian low. This response to reduced sea ice is consistent with previous modeling studies (e.g., McCusker et al., 2017). In contrast, in ADWs (Figure 4c; 61% of all winters), the circulation patterns associated with reduced sea ice mirror those observed in all winters (Figure 4a). These findings align with Blackport et al. (2019), who suggested based on surface temperature analysis that reduced sea ice in the CBS has only a weak impact on cold winters over North America, while anomalous large-scale atmospheric circulation in ADWs drives both the reduction of CBS ice and the occurrence of cold winters in North America.

In all winters, reduced sea ice is associated with the penetration of cyclones from the North Pacific into the CBS, resulting in an increase in track density and the mean intensity of storms from the northwestern North Pacific into the CBS (Figure 4d), bringing more energy and moisture into the CBS. Additionally, track density decreases from the southwestern North Pacific to the west coast of North America. This distribution of track density and mean intensity over the North Pacific is observed only in ADWs (Figures 4e and 4f). The pattern in all winters (Figure 4d) closely resembles that in ADWs (Figure 4f), suggesting that reduced sea ice is more strongly linked to storm tracks in ADWs than in IDWs. The penetration of storms into the CBS during ADWs amplifies warming and contributes to sea ice reduction in the region.

### 3.4. The Recent Trend in Atmospheric Circulation and Extratropical Storm Tracks

The track density and mean intensity of positive V extrema have not changed significantly in the Atlantic sector of the Arctic in recent decades (Figure 5a), suggesting that the storm-induced intrusion of warm and moist air has remained consistent. Additionally, there has been a decrease in track density from northeastern Europe to northern Siberia and the Laptev Sea (Figure 5a), a pattern similar to that observed during IDWs with reduced sea ice in the BKS (Figure 1e). The atmospheric circulation trend (Figure 5b) shows a strengthening of the anticyclonic circulation in the BKS and northern Russia, along with the development of cyclonic circulation over the Norwegian and North Seas. Furthermore, there is no robust evidence for a strengthening of the anticyclonic circulation over the eastern North Atlantic or the wave train structure during ADWs in recent decades (Figure 1c).

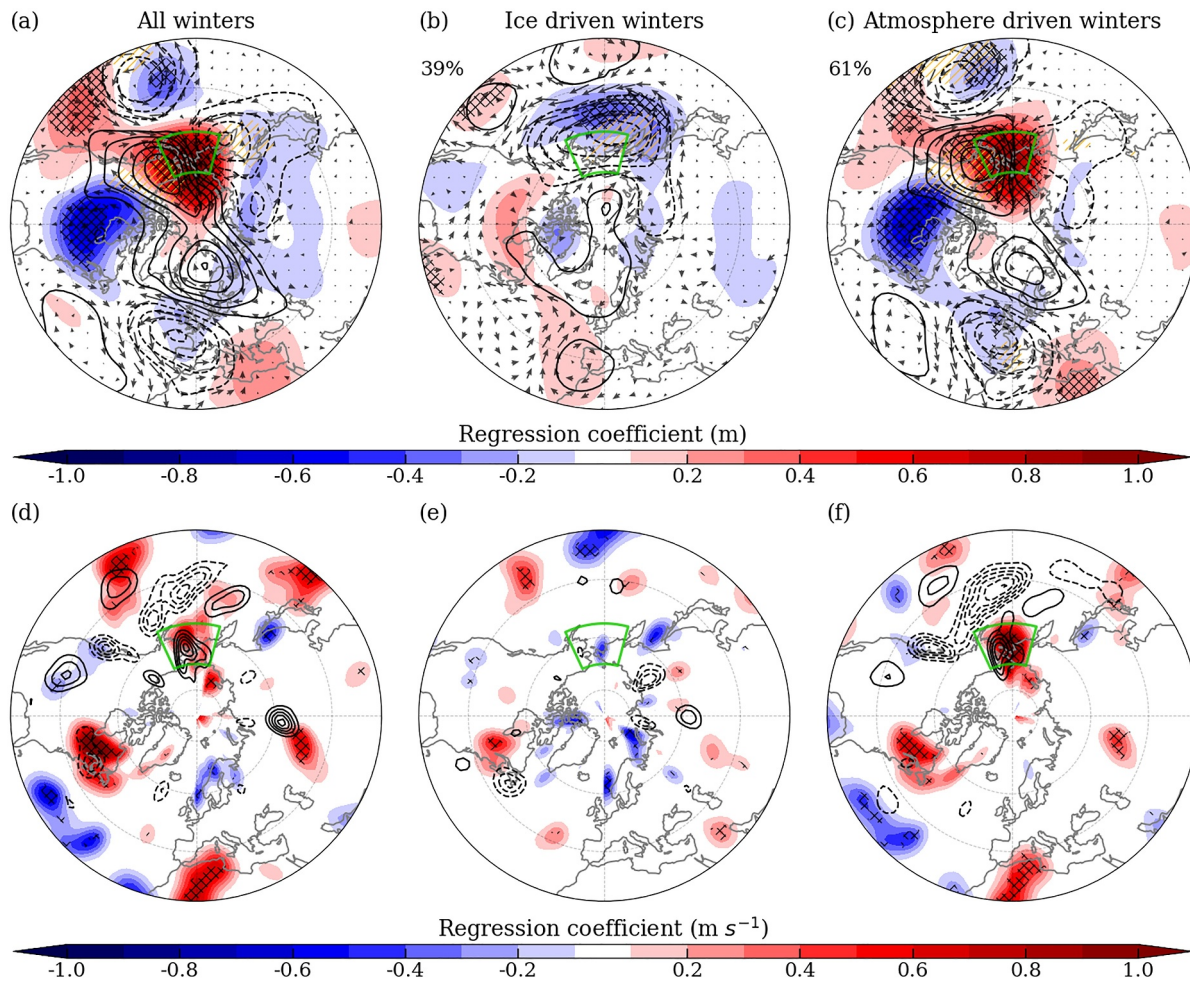


**Figure 4.** Same as Figure 1, but regressed on standardized reduced sea ice area (SIA) in the Chukchi-Bering Seas (CBS) (165°E and 155°W, 55–70°N, shown by the green polygon).

The track density and mean intensity of positive V extrema have increased from the northern North Pacific to the CBS (Figure 5a). While a similar pattern is observed only during ADWs with reduced sea ice in the CBS (Figure 4e), the atmospheric circulation trend (Figure 5b) does not resemble that seen in ADWs associated with reduced sea ice in the CBS (Figure 4c).

#### 4. Discussion and Conclusions

We investigated the response of atmospheric circulation and storm tracks to Arctic sea ice loss in three key subregions during winter, as well as the reciprocal influence of atmospheric circulation and storm tracks on Arctic sea ice. Building on the causality approach of Blackport et al. (2019), we considered two distinct conditions: (a) the Arctic sea ice driving the atmosphere (ice-driven winters—IDWs) and (b) the atmosphere driving the Arctic sea ice (atmosphere-driven winters—ADWs). In contrast to Blackport et al. (2019), who focused on sea level pressure and surface air temperature (which provide only insights into surface conditions), we analyzed geopotential height at 850 hPa. This allowed for a better understanding of circulation above the boundary layer. We also examined geopotential thickness between 1,000 and 500 hPa, which is a key component of the lower troposphere's thermal profile.

Notably, while Blackport et al. (2019) studied both the CBS and the BKS regions, we found similar results only for the CBS region. Our findings, therefore, do not support the notion of a minimal influence of Arctic sea ice loss on Asian winter cooling. Furthermore, we extended the study of Blackport et al. (2019) by analyzing track density

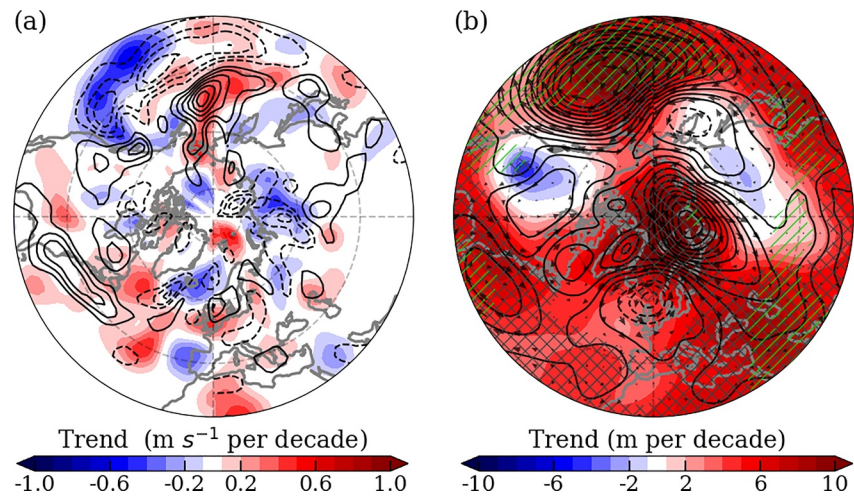


**Figure 5.** Linear trends of (a) track density (contours, 0.3 number density per unit area per month, where unit area is a  $5^\circ$  spherical cap) and mean intensity (shading,  $0.1 \text{ m s}^{-1}$  per decade) of storms, and (b) geopotential height at 850 hPa (contours, 1 m per decade) and geopotential thickness between 1,000 and 500 hPa (shading, 1 m per decade) during winter (DJF) from 1980 to 2023. Solid/dashed contours represent positive/negative trends (zero contour not shown). Green/black hatching indicates significant trends at the 90% confidence level after false discovery rate correction ( $\alpha_{\text{FDR}} = 0.1$ ) for geopotential height/thickness, track density, in Asia ( $70\text{--}130^\circ\text{E}$ ,  $25\text{--}90^\circ\text{N}$ ) and mean intensity.

and mean intensity of cyclones through a feature tracking method applied to the positive meridional wind component at 850 hPa.

The feedback mechanisms between sea ice and the atmosphere can occur across various timescales shorter than a season, as emphasized by Blackport et al. (2019). They found their conclusions to be robust to the use of seasonal or monthly means. They provided further confirmation of the robustness of their conclusions by performing some complementary analyses using the independent method of subseasonal lead-lag regressions. In a similar vein, to ensure the reliability of our findings, we incorporated a 1-month lead-lag analysis. Our results remain consistent whether we apply the 1-month lead-lag method or classify winters based on the signs of STHF and SIA anomalies. This consistency suggests that our classification scheme, particularly in the BKS, is effective in distinguishing whether sea ice is primarily driving atmospheric circulation or if atmospheric conditions are the primary driver of sea ice changes in winter. In IDWs, changes in sea ice primarily influence atmospheric circulation, or at least atmospheric circulation does not drive sea ice changes. In contrast, in ADWs, changes in atmospheric circulation are the main drivers of sea ice changes, or at least sea ice is not the dominant factor in atmospheric circulation variation.

Schematically summarizing our results in Figure 6, during IDWs, reduced sea ice in the BKS (Figure 6a) is linked to the development of an anomalous anticyclonic circulation over the BKS and northern Russia. This circulation pattern leads to a decrease in track density across northern Europe, the Ural Mountains, and the Laptev Sea, along with a reduction in the mean intensity of cyclones extending from northern Siberia to the Laptev Sea. In contrast, there is a local increase in both the mean intensity and the track density of cyclones within the BKS. Additionally, during IDWs, reduced sea ice in the CBS (Figure 6c) is associated with the development of a cyclonic circulation anomaly in the southern part of the region, along with a statistically nonsignificant increase in track density to the south of this cyclonic anomaly.

Luo et al. (2016) argued that a wave train structure originating from the North Atlantic and propagating toward Eurasia contributes to ice loss in the BKS. This wave train structure, characterized by the amplification of Ural blocking during the positive phase of the NAO, plays a key role in the significant decline of the sea ice in the BKS (Luo et al., 2016). Subsequent studies (e.g., Cai et al., 2022; Luo et al., 2017) have shown that this specific atmospheric circulation pattern serves as an effective moisture pathway from the midlatitude North Atlantic near the Gulf Stream to the BKS. The increased water vapor content in the atmosphere is crucial for both warming and the reduction of sea ice in the BKS. Our analysis suggests that this wave train structure is only present during ADWs (Figure 6b). It significantly contributes to an increase in track density in the Atlantic sector of the Arctic, while track

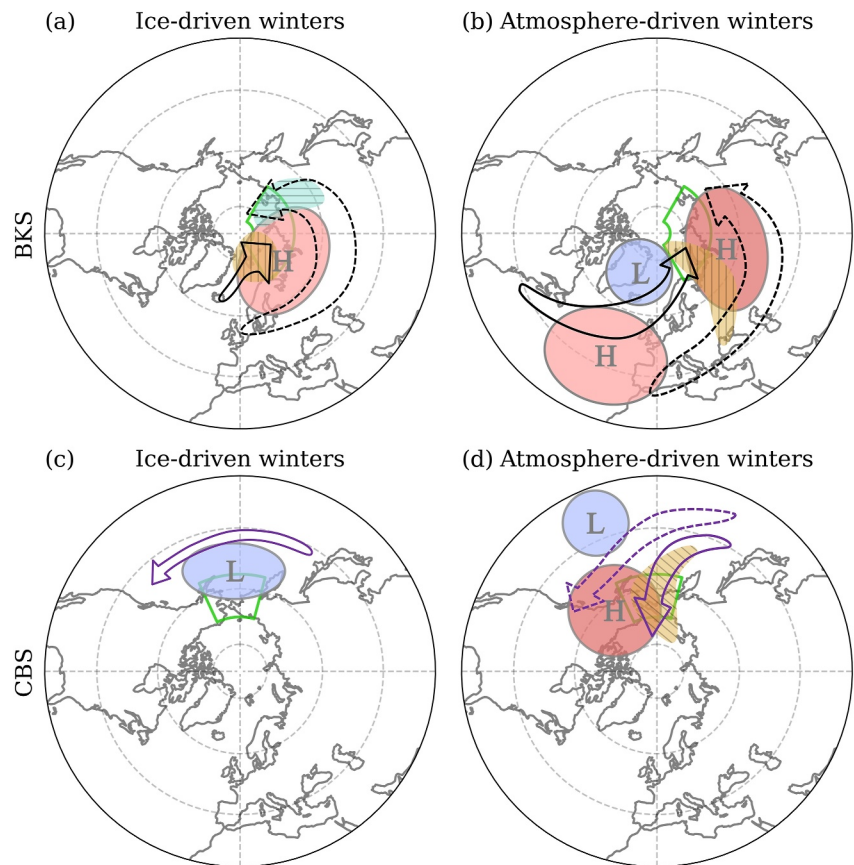


**Figure 6.** Schematic representation of geopotential height at 850 hPa (H for high and L for low), cyclone track density (arrows), and mean cyclone intensity (shaded hatching) associated with reduced sea ice in the Barents-Kara Sea (BKS) for (a) ice-driven winters (IDWs) and (b) atmosphere-driven winters (ADWs), and with reduced sea ice in the Chukchi-Bering Seas (CBS) for (c) IDWs and (d) ADWs. The letters H (L) or red (blue) circles represent areas of increased (decreased) geopotential height, while blue (brown) shaded hatching highlights regions of increased (decreased) mean cyclone intensity due to reduced sea ice. Solid (dashed) black arrows indicate areas of increased (decreased) cyclone track density. Track density and mean intensity are based on positive V extrema tracking. In IDWs, reduced sea ice in the BKS is associated with higher geopotential height over both the BKS and northern Russia, while reduced sea ice in the CBS is linked to lower geopotential height in the southern part of the region. In ADWs, reduced sea ice in the BKS is connected to a wave train structure that originates in the North Atlantic and propagates toward Eurasia, while reduced sea ice in the CBS is associated with higher geopotential height in the eastern CBS and northwestern Canada.

density decreases from southern Europe to northern Siberia (Figure 6b). Additionally, the mean intensity of cyclones is higher in the western part of the anticyclonic circulation in the BKS and lower in the eastern part (Figure 6b).

We argue that through a positive NAO pattern over the North Atlantic, this wave train structure enhances the cyclone-induced intrusion of heat and moisture into the BKS from the Atlantic sector. This increased intrusion of heat and moisture from cyclones contributes to amplified warming and further sea ice loss in the BKS, thus reinforcing the anticyclonic circulation over the BKS and North Eurasia. Therefore, the cyclone-driven intrusion of heat and moisture from the Atlantic sector into the Arctic promotes a circulation pattern that strengthens the connection between the positive NAO and the anticyclonic circulation in the BKS and northern Eurasia. In ADWs, reduced sea ice in the CBS is associated with the development of a stronger anticyclonic anomaly in the east of the CBS and the northwest of Canada (Figure 6d). This pattern contributes to the storm-induced intrusion of heat and moisture from the North Pacific into the CBS, while the storm-induced intrusion decreases from the western to the eastern North Pacific.

In IDWs, reduced sea ice in the BKS, CBS, and BDL has minimal effect on storm tracks in the NH. However, in ADWs, there is a substantial influx of storm tracks into the BKS and the CBS, which amplifies warming in these regions and leads to pronounced sea ice loss. The increase in the mean intensity of storms has a more substantial impact on melting the BDL sea ice than changes in track density.

Overall, in IDWs, reduced sea ice in the BKS can induce cooling in the midtroposphere over northeastern Asia, around 55°N. The mechanism behind this connection may be better understood by examining potential vorticity dynamics (e.g., Xie et al., 2020). Based on surface temperature analysis, Blackport et al. (2019) concluded that the loss of sea ice in the BKS has minimal influence on cold winters in Asia. However, to fully capture the signal of BKS ice loss, the entire tropospheric temperature must be considered. Our findings show that recent cooling in northeastern Asia peaks in the midtroposphere, which aligns with the effects of reduced sea ice in IDWs. Moreover, we observe that the latitude of maximum cooling in Asia during IDWs corresponds to the latitude of the maximum cooling trend. Thus, we argue that the loss of sea ice in the BKS has likely contributed to the development of colder winters in northeastern Asia, consistent with the results of Outten and Esau (2012) and in contrast to the conclusions of Blackport et al. (2019).

The atmospheric circulation trend pattern from the eastern North Atlantic to the BKS and northern Eurasia (Figure 5b) more closely resembles the pattern associated with reduced sea ice in the BKS during IDWs than in ADWs (Figure 6a). Additionally, there is no evidence of an increasing trend in track density or the mean intensity of positive V extrema in the North Atlantic sector of the Arctic (Figure 5a). We conclude that changes in atmospheric circulation are not the primary cause of recent sea ice loss in the BKS. Instead, the positive trend in storm-induced intrusion of warm, moist air into the CBS, driven by the strengthening of the anticyclonic circulation in the northeastern Pacific (Figure 5a), may have contributed to recent ice loss in the CBS (Figure 5b).

It is important to note that most studies have used the vertical component of relative vorticity or mean sea level pressure to identify storm tracks. However, storm track characteristics derived from these fields often differ from those identified using positive V extrema (e.g., Hoskins & Hodges, 2002). The use of V extrema specifically highlights the poleward advection of warm air in the east of cyclones, capturing a unique aspect of storm dynamics that traditional methods may not fully represent. The lack of a poleward shift in the downstream North Atlantic storm tracks during winter aligns with studies, such as Sun et al. (2022), which report no significant increase in atmospheric energy transport into the Arctic during this season.

This study has been guided by three key questions, providing insights into the complex interactions between Arctic sea ice, atmospheric circulation, and extratropical storm tracks. Our findings indicate that the recent sea ice loss in the BKS has not been driven by a significant increase in storm-induced heat and moisture intrusion or changes in atmospheric circulation. Instead, our results suggest that the recent loss of BKS sea ice may have contributed to colder winters in the midtroposphere of Central to Northeast Asia.

An important extension of this study will involve conducting a process-based analysis of cyclone impacts using model simulations and reanalysis. Additionally, modeling studies should evaluate whether the impact of sea ice loss in the BKS on Asian winter cooling is more pronounced at the surface or in the midtroposphere.

## Data Availability Statement

The ERA5 data set is publicly accessible through the Copernicus Climate Change Service Climate Data Store at <https://doi.org/10.24381/cds.bd0915c6> (Hersbach et al., 2023a), <https://doi.org/10.24381/cds.6860a573> (Hersbach et al., 2023b), and <https://doi.org/10.24381/cds.f17050d7> (Hersbach et al., 2023c). The cyclone tracking algorithm can be accessed at <https://gitlab.act.reading.ac.uk/track/track> (Hodges, 2020).

## References

- Ahmadi, R., & Alizadeh, O. (2023). The possible links between the Barents–Kara sea-ice area, ural blocking, and the North Atlantic oscillation. *Quarterly Journal of the Royal Meteorological Society*, 149(757), 3357–3372. <https://doi.org/10.1002/qj.4560>
- Alizadeh, O., & Lin, Z. (2021). Rapid Arctic warming and its link to the waviness and strength of the westerly jet stream over West Asia. *Global and Planetary Change*, 199, 103447. <https://doi.org/10.1016/j.gloplacha.2021.103447>
- Alizadeh, O., Sanei, A., & Babaei, M. (2024). Rapid Arctic warming and extreme weather events in eastern Europe and western to central Asia. *Climate Dynamics*, 62(9), 8889–8898. <https://doi.org/10.1007/s00382-024-07367-z>
- Arthun, M., Eldevik, T., & Smedsrud, L. H. (2019). The role of Atlantic heat transport in future Arctic winter sea ice loss. *Journal of Climate*, 32(11), 3327–3341. <https://doi.org/10.1175/jcli-d-18-0750.1>

## Acknowledgments

Open Access funding enabled and organized by Projekt DEAL.

- Asbjørnsen, H., Årthun, M., Skagseth, Ø., & Eldevik, T. (2020). Mechanisms underlying recent Arctic atlantification. *Geophysical Research Letters*, 47(15), e2020GL088036. <https://doi.org/10.1029/2020gl088036>
- Bengtsson, L., Hodges, K. I., & Keenlyside, N. (2009). Will extratropical storms intensify in a warmer climate? *Journal of Climate*, 22(9), 2276–2301. <https://doi.org/10.1175/2008jcli2678.1>
- Bengtsson, L., Hodges, K. I., & Roeckner, E. (2006). Storm tracks and climate change. *Journal of Climate*, 19(15), 3518–3543. <https://doi.org/10.1175/jcli3815.1>
- Blackport, R., Screen, J. A., van der Wiel, K., & Bintanja, R. (2019). Minimal influence of reduced Arctic sea ice on coincident cold winters in mid-latitudes. *Nature Climate Change*, 9, 697–704. <https://doi.org/10.1038/s41558-019-0551-4>
- Cai, M. (2006). Dynamical greenhouse-plus feedback and polar warming amplification. Part I: A dry radiative-transportive climate model. *Climate Dynamics*, 26(7–8), 661–675. <https://doi.org/10.1007/s00382-005-0104-6>
- Cai, Z., You, Q., Chen, H. W., Zhang, R., Chen, D., Chen, J., et al. (2022). Amplified wintertime Barents Sea warming linked to intensified Barents oscillation. *Environmental Research Letters*, 17(4), 044068. <https://doi.org/10.1088/1748-9326/ac5bb3>
- Catto, J. L., Shaffrey, L. C., & Hodges, K. I. (2011). Northern hemisphere extratropical cyclones in a warming climate in the HiGEM high-resolution climate model. *Journal of Climate*, 24(20), 5336–5352. <https://doi.org/10.1175/2011jcli4181.1>
- Clancy, R., Bitz, C. M., Edward, B. W., McGraw, M. C., & Cavallo, S. M. (2022). A cyclone-centered perspective on the drivers of asymmetric patterns in the atmosphere and sea ice during Arctic cyclones. *Journal of Climate*, 35, 73–89. <https://doi.org/10.1175/JCLI-D-21-0093.1>
- Dai, A., & Song, M. (2020). Little influence of Arctic amplification on mid-latitude climate. *Nature Climate Change*, 10(3), 231–237. <https://doi.org/10.1038/s41558-020-0694-3>
- Day, J. J., Holland, M. M., & Hodges, K. I. (2018). Seasonal differences in the response of Arctic cyclones to climate change in CESM1. *Climate Dynamics*, 50(9–10), 3885–3903. <https://doi.org/10.1007/s00382-017-3767-x>
- Deser, C., Tomas, R., Alexander, M., & Lawrence, D. (2010). The seasonal atmospheric response to projected Arctic sea ice loss in the late twenty-first century. *Journal of Climate*, 23(2), 333–351. <https://doi.org/10.1175/2009jcli3053.1>
- Deser, C., Walsh, J. E., & Timlin, M. S. (2000). Arctic sea ice variability in the context of recent atmospheric circulation trends. *Journal of Climate*, 13(3), 617–633. [https://doi.org/10.1175/1520-0442\(2000\)013<0617:asivit>2.0.co;2](https://doi.org/10.1175/1520-0442(2000)013<0617:asivit>2.0.co;2)
- Dufour, A., Zolina, O., & Gulev, S. K. (2016). Atmospheric moisture transport to the arctic: Assessment of reanalyses and analysis of transport components. *Journal of Climate*, 29(14), 5061–5081. <https://doi.org/10.1175/jcli-d-15-0559.1>
- Fearon, M. G., Doyle, J. D., Ryglicki, D. R., Finocchio, P. M., & Sprenger, M. (2021). The role of cyclones in moisture transport into the Arctic. *Geophysical Research Letters*, 48(4), e2020GL090353. <https://doi.org/10.1029/2020gl090353>
- Francis, J. A., & Vavrus, S. J. (2012). Evidence linking Arctic amplification to extreme weather in mid-latitudes. *Geophysical Research Letters*, 39(6), L06801. <https://doi.org/10.1029/2012gl01051000>
- Francis, J. A., & Vavrus, S. J. (2015). Evidence for a wavier jet stream in response to rapid Arctic warming. *Environmental Research Letters*, 10(1), 014005. <https://doi.org/10.1088/1748-9326/10/1/014005>
- Gong, T., Feldstein, S., & Lee, S. (2017). The role of downward infrared radiation in the recent arctic winter warming trend. *Journal of Climate*, 30(13), 4937–4949. <https://doi.org/10.1175/jcli-d-16-0180.1>
- Graversen, R. G., & Burtu, M. (2016). Arctic amplification enhanced by latent energy transport of atmospheric planetary waves. *Quarterly Journal of the Royal Meteorological Society*, 142(698), 2046–2054. <https://doi.org/10.1002/qj.2802>
- Hall, A. (2004). The role of surface albedo feedback in climate. *Journal of Climate*, 17(7), 1550–1568. [https://doi.org/10.1175/1520-0442\(2004\)017<1550:trosaf>2.0.co;2](https://doi.org/10.1175/1520-0442(2004)017<1550:trosaf>2.0.co;2)
- Hay, S., Priestley, M. D. K., Yu, H., Catto, J. L., & Screen, J. A. (2023). The effect of Arctic sea-ice loss on extratropical cyclones. *Geophysical Research Letters*, 50(17), e2023GL102840. <https://doi.org/10.1029/2023gl102840>
- He, S., Xu, X., Furevik, T., & Gao, Y. (2020). Eurasian cooling linked to the vertical distribution of Arctic warming. *Geophysical Research Letters*, 47(10), e2020GL087212. <https://doi.org/10.1029/2020gl087212>
- Hersbach, H., Bell, B., Berrisford, P., Biavati, G., Horányi, A., Muñoz Sabater, J., et al. (2023a). ERA5 hourly data on pressure levels from 1940 to present [Dataset]. *Copernicus Climate Change Service (C3S) Climate Data Store (CDS)*. <https://doi.org/10.24381/cds.bd0915c6>
- Hersbach, H., Bell, B., Berrisford, P., Biavati, G., Horányi, A., Muñoz Sabater, J., et al. (2023b). ERA5 monthly averaged data on pressure levels from 1940 to present [Dataset]. *Copernicus Climate Change Service (C3S) Climate Data Store (CDS)*. <https://doi.org/10.24381/cds.6860a573>
- Hersbach, H., Bell, B., Berrisford, P., Biavati, G., Horányi, A., Muñoz Sabater, J., et al. (2023c). ERA5 monthly averaged data on single levels from 1940 to present [Dataset]. *Copernicus Climate Change Service (C3S) Climate Data Store (CDS)*. <https://doi.org/10.24381/cds.f17050d7>
- Hersbach, H., Bell, B., Berrisford, P., Hirahara, S., Horányi, A., Muñoz-Sabater, J., et al. (2020). The ERA5 global reanalysis. *Quarterly Journal of the Royal Meteorological Society*, 146(730), 1999–2049. <https://doi.org/10.1002/qj.3803>
- Hodges, K. I. (1994). A general method for tracking analysis and its application to meteorological data. *Monthly Weather Review*, 122(11), 2573–2586. [https://doi.org/10.1175/1520-0493\(1994\)122<2573:agmfta>2.0.co;2](https://doi.org/10.1175/1520-0493(1994)122<2573:agmfta>2.0.co;2)
- Hodges, K. I. (1995). Feature tracking on the unit sphere. *Monthly Weather Review*, 123(12), 3458–3465. [https://doi.org/10.1175/1520-0493\(1995\)123<3458:ftotus>2.0.co;2](https://doi.org/10.1175/1520-0493(1995)123<3458:ftotus>2.0.co;2)
- Hodges, K. I. (1996). Spherical nonparametric estimators applied to the UGAMP model integration for AMIP. *Monthly Weather Review*, 124(12), 2914–2932. [https://doi.org/10.1175/1520-0493\(1996\)124<2914:sneatt>2.0.co;2](https://doi.org/10.1175/1520-0493(1996)124<2914:sneatt>2.0.co;2)
- Hodges, K. I. (1999). Adaptive constraints for feature tracking. *Monthly Weather Review*, 127(6), 1362–1373. [https://doi.org/10.1175/1520-0493\(1999\)127<1362:acfft>2.0.co;2](https://doi.org/10.1175/1520-0493(1999)127<1362:acfft>2.0.co;2)
- Hodges, K. I. (2020). TRACK tracking and analysis system for weather, climate and ocean data [Software]. <https://gitlab.act.reading.ac.uk/track/track>
- Honda, M., Inoue, J., & Yamane, S. (2009). Influence of low Arctic sea-ice minima on anomalously cold Eurasian winters. *Geophysical Research Letters*, 36(8), L08707. <https://doi.org/10.1029/2008gl037079>
- Hoskins, B. J., & Hodges, K. I. (2002). New perspectives on the Northern Hemisphere winter storm tracks. *Journal of the Atmospheric Sciences*, 59(6), 1041–1061. [https://doi.org/10.1175/1520-0469\(2002\)059<1041:npoth>2.0.co;2](https://doi.org/10.1175/1520-0469(2002)059<1041:npoth>2.0.co;2)
- Hoskins, B. J., & Hodges, K. I. (2005). A new perspective on Southern Hemisphere storm tracks. *Journal of Climate*, 18(20), 4108–4129. <https://doi.org/10.1175/jcli3570.1>
- Hoskins, B. J., & Hodges, K. I. (2019a). The annual cycle of northern hemisphere storm tracks. Part I: Seasons. *Journal of Climate*, 32(6), 1743–1760. <https://doi.org/10.1175/jcli-d-17-0870.1>
- Hoskins, B. J., & Hodges, K. I. (2019b). The annual cycle of Northern Hemisphere storm tracks. Part II: Regional detail. *Journal of Climate*, 32(6), 1761–1775. <https://doi.org/10.1175/jcli-d-17-0871.1>
- Inoue, J., Hori, M. E., & Takaya, K. (2012). The role of barents sea ice in the wintertime cyclone track and emergence of a warm-Arctic cold-Siberian anomaly. *Journal of Climate*, 25(7), 2561–2569. <https://doi.org/10.1175/jcli-d-11-00449.1>

- Ivanov, V., Alexeev, V., Koldunov, N. V., Repina, I., Sandø, A. B., Smedsrud, L. H., & Smirnov, A. (2016). Arctic ocean heat impact on regional ice decay: A suggested positive feedback. *Journal of Physical Oceanography*, *46*(5), 1437–1456. <https://doi.org/10.1175/jpo-d-15-0144.1>
- Jenkins, M., & Dai, A. (2021). The impact of sea-ice loss on Arctic climate feedbacks and their role for Arctic amplification. *Geophysical Research Letters*, *48*(15), e2021GL094599. <https://doi.org/10.1029/2021gl094599>
- Lee, S., Gong, T., Feldstein, S. B., Screen, J. A., & Simmonds, I. (2017). Revisiting the cause of the 1989–2009 Arctic surface warming using the surface energy budget: Downward infrared radiation dominates the surface fluxes. *Geophysical Research Letters*, *44*(20), 10654–10661. <https://doi.org/10.1002/2017gl075375>
- Liu, C., & Barnes, E. A. (2015). Extreme moisture transport into the Arctic linked to Rossby wave breaking. *Journal of Geophysical Research: Atmospheres*, *120*(9), 3774–3788. <https://doi.org/10.1002/2014jd022796>
- Luo, B., Luo, D., Wu, L., Zhong, L., & Simmonds, I. (2017). Atmospheric circulation patterns which promote winter Arctic sea ice decline. *Environmental Research Letters*, *12*(5), 054017. <https://doi.org/10.1088/1748-9326/aa69d0>
- Luo, D., Luo, B., Zhang, W., Zhuo, W., Simmonds, I., & Yao, Y. (2024). Arctic amplification-induced intensification of planetary wave modulational instability: A simplified theory of enhanced large-scale waviness. *Quarterly Journal of the Royal Meteorological Society*, *150*(762), 2888–2905. <https://doi.org/10.1002/qj.4740>
- Luo, D., Xiao, Y., Yao, Y., Dai, A., Simmonds, I., & Franzke, C. L. E. (2016). Impact of ural blocking on winter warm Arctic-cold Eurasian anomalies. Part I: Blocking-induced amplification. *Journal of Climate*, *29*(11), 3925–3947. <https://doi.org/10.1175/jcli-d-15-0611.1>
- McCusker, K. E., Kushner, P. J., Fyfe, J. C., Sigmond, M., Kharin, V. V., & Bitz, C. M. (2017). Remarkable separability of circulation response to Arctic sea ice loss and greenhouse gas forcing. *Geophysical Research Letters*, *44*(15), 7955–7964. <https://doi.org/10.1002/2017gl074327>
- Mori, M., Kosaka, Y., Watanabe, M., Nakamura, H., & Kimoto, M. (2019). A reconciled estimate of the influence of Arctic sea-ice loss on recent Eurasian cooling. *Nature Climate Change*, *9*(2), 123–129. <https://doi.org/10.1038/s41558-018-0379-3>
- Mori, M., Watanabe, M., Shiogama, H., Inoue, J., & Kimoto, M. (2014). Robust Arctic sea-ice influence on the frequent Eurasian cold winters in past decades. *Nature Geoscience*, *7*(12), 869–873. <https://doi.org/10.1038/ngeo2277>
- Outten, S. D., & Esau, I. (2012). A link between Arctic sea ice and recent cooling trends over Eurasia. *Climatic Change*, *110*(3–4), 1069–1075. <https://doi.org/10.1007/s10584-011-0334-z>
- Petoukhov, V., & Semenov, V. A. (2010). A link between reduced Barents-Kara sea ice and cold winter extremes over northern continents. *Journal of Geophysical Research*, *115*(D21), D21111. <https://doi.org/10.1029/2009jd013568>
- Pithan, F., & Mauritsen, T. (2014). Arctic amplification dominated by temperature feedbacks in contemporary climate models. *Nature Geoscience*, *7*(3), 181–184. <https://doi.org/10.1038/ngeo2071>
- Rantanen, M., Karpechko, A. Y., Lipponen, A., Nordling, K., Hyvärinen, O., Ruosteenoja, K., et al. (2022). The Arctic has warmed nearly four times faster than the globe since 1979. *Communications Earth and Environment*, *3*(1), 168. <https://doi.org/10.1038/s43247-022-00498-3>
- Rinke, A., Maturilli, M., Graham, R. M., Matthes, H., Handorf, D., Cohen, L., et al. (2017). Extreme cyclone events in the Arctic: Wintertime variability and trends. *Environmental Research Letters*, *12*(9), 094006. <https://doi.org/10.1088/1748-9326/aa7def>
- Sato, K., Inoue, J., & Watanabe, M. (2014). Influence of the Gulf stream on the Barents Sea ice retreat and Eurasian coldness during early winter. *Environmental Research Letters*, *9*(8), 084009. <https://doi.org/10.1088/1748-9326/9/8/084009>
- Serreze, M. C., Barrett, A. P., Stroeve, J. C., Kindig, D. N., & Holland, M. M. (2009). The emergence of surface-based Arctic amplification. *The Cryosphere*, *3*(1), 11–19. <https://doi.org/10.5194/tc-3-11-2009>
- Simmonds, I., Burke, C., & Keay, K. (2008). Arctic climate change as manifest in cyclone behavior. *Journal of Climate*, *21*(22), 5777–5796. <https://doi.org/10.1175/2008jcli2366.1>
- Simmonds, I., & Govekar, P. D. (2014). What are the physical links between Arctic sea ice loss and Eurasian winter climate? *Environmental Research Letters*, *9*(10), 101003. <https://doi.org/10.1088/1748-9326/9/10/101003>
- Simmonds, I., & Keay, K. (2009). Extraordinary September Arctic sea ice reductions and their relationships with storm behavior over 1979–2008. *Geophysical Research Letters*, *36*(19), L19715. <https://doi.org/10.1029/2009gl039810>
- Simmonds, I., & Li, M. (2021). Trends and variability in polar sea ice, global atmospheric circulations, and baroclinicity. *Annals of the New York Academy of Sciences*, *1504*(1), 167–186. <https://doi.org/10.1111/nyas.14673>
- Sorteberg, A., & Walsh, J. E. (2008). Seasonal cyclone variability at 70°N and its impact on moisture transport into the Arctic. *Tellus*, *60*(3), 570–586. <https://doi.org/10.1111/j.1600-0870.2008.00314.x>
- Stroeve, J., & Notz, D. (2018). Changing state of Arctic sea ice across all seasons. *Environmental Research Letters*, *13*(10), 103001. <https://doi.org/10.1088/1748-9326/aade56>
- Sun, W., Liang, Y., Bi, H., Zhao, Y., Meng, J., & Zhang, J. (2022). Insight on poleward moisture and energy transport into the Arctic from ERA5. *Atmosphere*, *13*(4), 616. <https://doi.org/10.3390/atmos13040616>
- Tang, Q., Zhang, X., Yang, X., & Francis, J. A. (2013). Cold winter extremes in northern continents linked to Arctic sea ice loss. *Environmental Research Letters*, *8*(1), 014036. <https://doi.org/10.1088/1748-9326/8/1/014036>
- Wilks, D. S. (2016). The stippling shows statistically significant grid points”: How research results are routinely overstated and overinterpreted, and what to do about it. *Bulletin of the American Meteorological Society*, *97*(12), 2263–2273. <https://doi.org/10.1175/bams-d-15-00267.1>
- Woods, C., & Caballero, R. (2016). The role of moist intrusions in winter arctic warming and sea ice decline. *Journal of Climate*, *29*(12), 4473–4485. <https://doi.org/10.1175/jcli-d-15-0773.1>
- Woods, C., Caballero, R., & Svensson, G. (2013). Large-scale circulation associated with moisture intrusions into the Arctic during winter. *Geophysical Research Letters*, *40*(17), 4717–4721. <https://doi.org/10.1002/grl.50912>
- Xie, Y., Wu, G., Liu, Y., & Huang, J. (2020). Eurasian cooling linked with arctic warming: Insights from PV dynamics. *Journal of Climate*, *33*(7), 2627–2644. <https://doi.org/10.1175/jcli-d-19-0073.1>
- Xu, M., Tian, W., Zhang, J., Screen, J. A., Zhang, C., & Wang, Z. (2023). Important role of stratosphere-troposphere coupling in the Arctic mid-to-upper tropospheric warming in response to sea-ice loss. *Npj Climate and Atmospheric Science*, *6*(1), 9. <https://doi.org/10.1038/s41612-023-00333-2>
- Yu, Q., Wu, B., & Zhang, W. (2024). The atmospheric connection between the Arctic and Eurasia is underestimated in simulations with prescribed sea ice. *Communications Earth and Environment*, *5*(1), 435. <https://doi.org/10.1038/s43247-024-01605-2>
- Zahn, M., Akperov, M., Rinke, A., Feser, F., & Mokhov, I. I. (2018). Trends of cyclone characteristics in the Arctic and their patterns from different reanalysis data. *Journal of Geophysical Research: Atmospheres*, *123*(5), 2737–2751. <https://doi.org/10.1002/2017jd027439>
- Zappa, G., Shaffrey, L. C., & Hodges, K. I. (2013). The ability of CMIP5 models to simulate North Atlantic extratropical cyclones. *Journal of Climate*, *26*(15), 5379–5396. <https://doi.org/10.1175/jcli-d-12-00501.1>
- Zhang, J., Lindsay, R., Schweiger, A., & Steele, M. (2013). The impact of an intense summer cyclone on 2012 Arctic sea ice retreat. *Geophysical Research Letters*, *40*(4), 720–726. <https://doi.org/10.1002/grl.50190>

- Zhang, P., Wu, Y., Simpson, I. R., Smith, K. L., Zhang, X., De, B., & Callaghan, P. (2018). A stratospheric pathway linking a colder Siberia to Barents-Kara Sea sea ice loss. *Science Advances*, *4*(7), eaat6025. <https://doi.org/10.1126/sciadv.aat6025>
- Zhuo, W., Yao, Y., Luo, D., Simmonds, I., & Huang, F. (2023). The key atmospheric drivers linking regional Arctic amplification with East Asian cold extremes. *Atmospheric Research*, *283*, 106557. <https://doi.org/10.1016/j.atmosres.2022.106557>